THE ASTROPHYSICAL JOURNAL, 380:541–549, 1991 October 20

RADIATIVE WIDTHS AND SPLITTING OF CYCLOTRON LINES IN SUPERSTRONG MAGNETIC FIELDS

G. G. PAVLOV[1]
Pennsylvania State University and Ioffe Institute of Physics and Technology

V. G. BEZCHASTNOV[1]
Ioffe Institute of Physics and Technology

P. MÉSZÁROS[2]
Pennsylvania State University and Harvard-Smithsonian Center for Astrophysics

AND

S. G. ALEXANDER[3]
Pennsylvania State University

Received 1990 December 26; accepted 1991 April 30

ABSTRACT

We calculate the radiative line widths of the Landau levels in a superstrong magnetic field and give simple analytic expressions and fits for these which are valid over a wide range of the principal quantum number and the magnetic field strength. If one does not allow for QED corrections, all levels but the first are doubly degenerate, corresponding to the two possible spin projections. However, the interaction with the QED vacuum removes this degeneracy, leading to an energy splitting of each level which exceeds the radiative line width for low Landau levels if the magnetic field is not too large ($B \lesssim 10^{13}$ G). We present estimations of the splitting in various limits as a function of field strength and Landau number. The possibility of observing this splitting in accreting X-ray pulsars and in gamma-ray bursters is discussed.

Subject headings: atomic processes — magnetic fields — radiation mechanisms — stars: neutron — X-ray: spectra

1. INTRODUCTION

Cyclotron lines are important diagnostic tools for neutron star astrophysics, allowing a direct determination of the magnetic field, and line profiles give information about the physical conditions in the radiating region. In the X-ray range, these lines have been discovered in several accreting pulsars (Her X-1, 4U 0115+63, 4U 1538−52, X0331+53, e.g. Trümper et al. 1978; Wheaton, et al. 1979; White et al. 1983; Clark et al. 1990; Mihara et al. 1990; Nagase et al. 1991; Makishima et al. 1991), and in a number of gamma-ray bursters (GB 870303, GB 880205, GB 890929, and earlier data from *Konus*, e.g. Murakami et al. 1988; Yoshida et al. 1990; Mazets et al. 1981). Cyclotron lines arise mainly as a result of scattering, or with smaller probability by emission and absorption, involving free electron transitions between quantized energy levels in the presence of the superstrong magnetic field. In such a field, the energy of an electron or positron is given by the Landau levels, characterized by the principal quantum number $n = 0, 1, 2, \ldots$ and the normalized magnetic field strength $b = \hbar\omega_c/m_e c^2 = B/B_Q$, where $\omega_c = eB/m_e c$ is the cyclotron energy and $B_Q = m^2c^3/e\hbar = 4.413 \times 10^{13}$ G is the critical QED field. In units of the electron rest energy, the relativistic expression for the energy is

$$\varepsilon = \varepsilon_n(p_z) = \sqrt{1 + 2nb + p_z^2}\ , \tag{1}$$

where the first term represents the rest energy, the second is the transverse energy, and the third is the longitudinal energy, p_z being the $e^{\pm}$ momentum in units of $m_e c$ projected onto the direction of the magnetic field. The excited levels $n > 0$ are usually considered to be twice degenerate over spin projections, with two Dirac bispinor eigenfunctions corresponding to each level. The coupling of the electrons to the radiation field by the interaction Hamiltonian H_I leads to a natural broadening of the excited levels. A less widely appreciated fact, however, is that the same interaction also leads to a finite splitting and shifting of each level, which under a range of conditions can exceed the natural line width and may be observable with currently planned detectors.

Although as a rule, in normal astrophysical situations, the natural widths are small compared to the Doppler widths, they are needed for the accurate calculation of many radiative processes and for the calculation of realistic line profiles. For instance, they are needed to avoid the singularities which appear in the cyclotron emission/absorption spectrum and in the magnetic one-photon pair creation/annihilation spectrum, at angles θ between $\boldsymbol{B}$ and $\boldsymbol{k}$ close to $\pi/2$ (e.g., Herold et al. 1982a; Pavlov 1986; Harding 1986; Bezchastnov & Pavlov 1990). They are also necessary in order to treat appropriately the resonances in the QED magnetic Compton scattering cross section (e.g., Daugherty & Harding 1986; Bussard, Alexander & Mészáros 1986; Harding & Preece 1989). These resonances appear at energies $\omega \simeq n\omega_c$, the exact energies and Doppler widths depending on the angles of the incoming and

[1] Ioffe Institute of Physics and Technology, USSR Academy of Sciences, 194064 Leningrad, USSR.
[2] Pennsylvania State University, 525 Davey Laboratory, University Park, PA 16802.
[3] Physics Department, Saint Bonaventure University, Saint Bonaventure, NY 14778.

outgoing photons respect to $\boldsymbol{B}$. General expressions for the natural width were derived by Herold et al. (1982a, b), Latal et al. (1986), and Mitrofanov & Pozaneneko (1987). To calculate these widths requires integrations over θ and sums over all Landau levels $n' < n$ of complicated expressions, which can be cumbersome and time consuming when n is not small. However, simple approximate expressions can be obtained for the widths in various limiting cases, and it is obviously useful to derive simple interpolation formulae that match these limiting cases and are sufficiently accurate over a wide range of parameters.

The energy shift of the Landau levels is intimately connected to the natural line broadening, these quantities being the real and imaginary parts of the complex radiative shift (see, e.g., Akhiezer & Berestetskii 1981). The shifts are generally dependent on the sign of the $e^{\pm}$ spin projection ζ onto $\boldsymbol{B}$, $\zeta = \pm 1$. This means that the shift can remove the degeneracy of the Landau levels, leading to a finite energy split of each level, if the distance between the shifted sublevels exceeds the natural width. The possibility of measuring this shift in the high-energy spectrum of magnetized neutron stars would be of great interest, and for this it is necessary to calculate the shifts and widths over a wide range of the parameters n and $b = B/B_Q$. Notice that it is not necessary to include in these calculations the dependence on the longitudinal momentum of the electron or positron p_z, since the value of the widths and splitting for $p_z \neq 0$ can be obtained from those for $p_z = 0$ through a Lorentz transformation (Herold et al. 1982a).

In § 2 we consider the various limiting values for the radiative width, and we compare the results of these and the interpolation formulae with those we obtain from numerical calculations of the exact relativistic expressions. In § 3 we discuss the results on the splitting of the Landau levels, giving both exact and approximate expressions, and we compare these with the corresponding widths as a function of n and b. The results and their observational implications are discussed in § 4.

2. NATURAL BROADENING OF THE LANDAU LEVELS

The natural width Γ_n^{ζ} of the electron state $|n, \zeta, p_z = 0\rangle$ can be defined as the sum of the partial widths:

$$\Gamma_n^{\zeta} = \sum_{n'<n} \Gamma_{nn'}^{\zeta} = \sum_{n'<n} \sum_{\zeta'=\pm 1} \Gamma_{nn'}^{\zeta\zeta'} , \tag{2}$$

where $\zeta = \pm 1$ is the sign of the spin projection onto the magnetic field. General equations for $\Gamma_{nn'}^{\zeta}$ were obtained, e.g., by Herold et al. (1982a) (their eq. [17]). This can be written in units of $m_e c^2$ as

$$\begin{aligned}\Gamma_{nn'}^{\zeta} = \frac{\alpha}{2}\int_0^{\pi/2} d\theta \frac{\omega \sin\theta}{\varepsilon_n\sqrt{\varepsilon_n^2 - 2(n-n')b\sin^2\theta}} &\{[(\varepsilon_n - \zeta)(\varepsilon_n + \zeta - \omega)I_{n,n'}^2(u) + (\varepsilon_n + \zeta)(\varepsilon_n - \zeta - \omega)I_{n-1,n'-1}^2(u)]\sin^2\theta \\ &+ [(\varepsilon_n + \zeta)(\varepsilon_n - \zeta - \omega)I_{n-1,n}^2(u) + (\varepsilon_n - \zeta)(\varepsilon_n + \zeta - \omega)I_{n,n'-1}^2(u)](1 + \cos^2\theta) \\ &+ 2\sqrt{2nb}\,\omega[I_{n,n'}(u)I_{n-1,n'}(u) + I_{n,n'-1}(u)I_{n-1,n'-1}(u)]\sin\theta\cos^2\theta \\ &+ 4\sqrt{nn'}\,b[I_{n-1,n'}(u)I_{n,n'-1}(u) + I_{n,n'}(u)I_{n-1,n'-1}(u)]\sin^2\theta\} ,\end{aligned} \tag{3}$$

where

$$\omega = \frac{1}{\sin^2\theta}\left[\varepsilon_n - \sqrt{\varepsilon_n^2 - 2(n-n')b\sin^2\theta}\right] = \omega_{nn'}(\theta) \tag{4}$$

is the dimensionless frequency of a photon irradiated at the transition $n \rightarrow n'$ at an angle θ, $\varepsilon_n \equiv \varepsilon_n(p_z = 0) = \sqrt{1 + 2nb}$ is the energy, $\alpha = e^2/\hbar c$ is the fine-structure constant, and $I_{n,n'}(u)$ are the functions constructed from the associated Laguerre polynomials

$$I_{n,n'}(u) = (-1)^n (n!\,n'!)^{-1/2} e^{u/2} u^{(n-n')/2} \frac{\partial^n}{\partial u^n}(u^{n'} e^{-u}) , \tag{5}$$

whose argument is $u = (\omega^2 \sin^2\theta)/2b$. The expression for the width (eq. [3]) simplifies considerably in the following limiting cases.

Case A: Nonrelativistic limit, $nb \ll 1$ (electron transverse energy $\varepsilon_\perp \ll m_e c^2$).—In this case one obtains (Melrose & Zheleznyakov 1981; Herold et al. 1982)

$$\Gamma_{nn'}^{-} = \alpha b^{n-n'+1} \frac{(n-n'+1)(n-n')^{2(n-n')}2^{n-n'+1}n!}{(2n-2n'+1)!\,n'!} , \tag{6a}$$

$$\Gamma_{nn'}^{+} = \frac{n'}{n}\Gamma_{nn'}^{-} \qquad (\text{if}\quad n' > 0) , \tag{6b}$$

$$\Gamma_{n0}^{+} = \alpha b^{n+2} \frac{n^{2n+1}2^n(n+1)!}{(2n+1)!} \qquad (\text{if}\quad n' = 0) . \tag{6c}$$

In these equations, the main contribution to Γ_n^{ζ} clearly comes from the terms $n' = n - 1$, i.e.,

$$\Gamma_n^{-} = \tfrac{4}{3}\alpha n b^2 , \tag{7a}$$

$$\Gamma_n^{+} = \tfrac{4}{3}\alpha(n-1)b^2 \qquad (\text{if}\quad n > 1) , \tag{7b}$$

$$\Gamma_1^{+} = \tfrac{2}{3}\alpha b^3 . \tag{7c}$$

For some applications, one needs the spin-averaged width $\Gamma_n = (\Gamma_n^{+} + \Gamma_n^{-})/2$. In the nonrelativistic limit this is given by

$$\Gamma_n = \tfrac{4}{3}\alpha(n - \tfrac{1}{2})b^2 , \tag{8a}$$

which depends on n, whereas the difference

$$\Delta\Gamma_n = \Gamma_n^- - \Gamma_n^+ = \tfrac{4}{3}\alpha b^2 \tag{8b}$$

is independent of n. Obviously this nonrelativistic limit can only be achieved in nonrelativistic magnetic fields $b \ll 1$.

By increasing n at a fixed $b \ll 1$, one reaches the ultrarelativistic limit $n \gg b^{-1} \gg 1$. In this limit all the terms n, n', and $n - n'$ contributing to Γ_n^ζ are very large compared to unity, and one can neglect the quantization of the Landau levels (replacing the sums over n' by integrals), using the asymptotic quasi-classical expressions for the $I_{n,n'}(u)$ in terms of McDonalds functions (see, e.g., Sokolov & Ternov 1986). Integrating these over θ, we obtain

$$\Gamma_n^{\zeta\zeta'} = \frac{\sqrt{3}}{4\pi}\,\alpha b \int_0^\infty \frac{dv}{(1+\eta v)^2}\left\{\frac{1+\zeta\zeta'}{2}\left[2\int_v^\infty K_{5/2}(\xi)d\xi + \frac{\eta^2 v^2}{1+\eta v}\,K_{2/3}(v) - \zeta\eta v\left(1+\frac{1}{1+\eta v}\right)K_{1/3}(v)\right]\right.$$
$$\left. + \frac{1-\zeta\zeta'}{2}\,\frac{\eta^2 v^2}{1+\eta v}\,[K_{2/3}(v) + \zeta K_{1/3}(v)]\right\}, \tag{9a}$$

where

$$\eta \equiv \tfrac{3}{2} b\sqrt{2nb} = \tfrac{3}{2}\sqrt{2nb^3}\,. \tag{9b}$$

Summing equation (9a) over ζ', one obtains

$$\Gamma_n^\zeta = \frac{\sqrt{3}}{2\pi}\,\alpha b \int_0^\infty \frac{dv}{(1+\eta v)}\left[\int_v^\infty K_{5/3}(\xi)d\xi + \frac{\eta^2 v^2}{1+\eta v}\,K_{2/3}(v) - \zeta\,\frac{\eta v}{1+\eta v}\,K_{1/3}(v)\right]. \tag{10}$$

Both $\Gamma_n^{\zeta\zeta'}$ and Γ_n^ζ depend on n only through the parameter η defined in equation (9b), which is determined by the ratio of the characteristic energy of the synchrotron photons, $bp_\perp \varepsilon \sim b\varepsilon\sqrt{nb}$, to the electron energy ε. When the parameter η is not small, quantum effects such as the electron recoil and spin-flip transitions are important, whereas in the opposite limit of $\eta \ll 1$ one is dealing with the classical synchrotron limit. We can therefore consider two additional limiting cases.

Case B: Ultrarelativistic quasi-classical limit, $b^{-1} \ll n \ll b^{-3}$, ($\eta \ll 1$).—In this limit, a direct evaluation of the integrals in equation (10), expanded up to terms of order η, yields the value

$$\Gamma_n^\zeta = \frac{5}{2\sqrt{3}}\,\alpha b\left(1 - \frac{8}{5\sqrt{3}}\sqrt{2nb^3} - \zeta\,\frac{3}{10}\sqrt{2nb^3}\right) \simeq 1.44\alpha b(1 - 1.3\sqrt{nb^3} - \zeta 0.42\sqrt{nb^3})\,. \tag{11}$$

We see that the spin-averaged width Γ_n is almost independent of n, whereas the difference $\Delta\Gamma_n$, which is associated with small quantum effects, grows proportionally with $n^{1/2}$.

Case C: Ultrarelativistic Quantum Limit, $n \gg b^{-3}$, ($\eta \gg 1$).—In this limit it is only the $v \ll 1$ values that contribute significantly to the integrals for Γ_n^ζ. Using the corresponding expansions of the MacDonald functions and evaluating the integrals, one obtains

$$\Gamma_n^\zeta = \frac{14\Gamma(2/3)\alpha b}{3^{7/3}(2nb^3)^{1/6}}\left[1 - \zeta\,\frac{\Gamma(1/3)}{14 \times 3^{1/3}\Gamma(2/3)(2nb)^{1/6}}\right] = \frac{1.30\alpha b}{(nb^3)^{1/6}}\left[1 - \zeta\,\frac{0.087}{(nb^3)^{1/6}}\right]. \tag{12}$$

From this we see that both Γ_n and $\Delta\Gamma_n$ decrease slowly with n. The results for the limiting case A, B, C match each other at $n \sim b^{-1}$ and $n \sim b^{-3}$. This allows one to write down a simple low-order interpolation formula which has the correct limiting behaviors:

$$\Gamma_n^\zeta = \frac{a_{1\zeta}[n - (1+\zeta)/2]\alpha b^2}{[\![1 + \{a_{2\zeta}[n - (1+\zeta)/2]b\}^{a_{3\zeta}}]\!]^{1/a_{3\zeta}}[1 + (a_{4\zeta}nb^3)^{a_{5\zeta}}]^{1/6a_{5\zeta}}}\,. \tag{13}$$

We calculated Γ_n^ζ from equation (3) for $b = 0.01$, 0.02, 0.03, 0.06, 0.1, 0.2, 0.3, and 0.6 for $n = 1$–1000 with an accuracy of 0.01% and fitted the results using equation (13) with the $a_{i\zeta}$ as fitting parameters. Values of these parameters for the best fit in the region $b = 0.01$–0.6, $n = 2$–1000 are given in Table 1.

The relative errors in this fitting are maximal (11% for Γ_n^{-1} and 15% for Γ_n^{+1}) for $n = 2$ at the lowest and highest values of the magnetic field used here in the fitting procedure. If one narrows the field limits, the maximum errors diminish significantly (6% for Γ_n^{-1} and 7% for Γ_n^{+1} in the range $0.03 \le b \le 0.3$).

To fit the widths with higher accuracy, one can express the $a_{i\zeta}$ in equation (13) as a quadratic function of the field,

$$a_{i\zeta} = c_i^\zeta + d_i^\zeta b + e_i^\zeta b^2\,, \tag{14}$$

considering c_i^ζ, d_i^ζ, and e_i^ζ as new fitting parameters. The best fit in the range $b = 0.01$–0.6, $n = 2$–1000 was obtained with the parameters given in Table 2.

TABLE 1

PARAMETERS $a_{i\zeta}$

ζ	$a_{1\zeta}$	$a_{2\zeta}$	$a_{3\zeta}$	$a_{4\zeta}$	$a_{5\zeta}$
−1.........	1.568	0.952	0.701	6.518	0.299
+1.........	1.740	0.760	0.673	49.61	0.197

TABLE 2

PARAMETERS c_i^ζ, d_i^ζ, e_i^ζ

i	c_i^{-1}	d_i^{-1}	e_i^{-1}	c_i^{+1}	d_i^{+1}	e_i^{+1}
1..........	1.385	−1.077	1.473	1.381	−2.419	3.167
2..........	1.095	0.3025	−0.8404	1.024	−0.7523	0.5282
3..........	0.8447	−0.2156	0.00656	0.8421	−0.2652	0.04603
4..........	0.7933	−3.601	5.550	0.3632	−1.924	3.109
5..........	0.4779	−0.5903	0.3185	0.2458	−0.1617	0.02845

The typical accuracy of this improved fit is a few tenths of a percent, the maximum errors being 2.5% for Γ_n^{-1} (at $n = 2$, $b = 0.01$) and 3.1% for Γ_n^{+1} (for $n = 2$, $b = 0.3$). The maximum errors decrease as the field limits are narrowed (e.g., 1.7% for Γ_n^{-1} and 2.1% for Γ_n^{+1} in the range $0.03 \leq b \leq 0.3$). Examples of these fits are shown with full lines in Figure 1 for $b = 0.03$, 0.1, 0.3. To demonstrate the difference between the exact quantum results of equation (3) and the ultrarelativistic limit of equation (10), we have also plotted in Figure 1 the widths from the latter as dot-dashed lines. We see that the difference can be significant even for very high Landau levels.

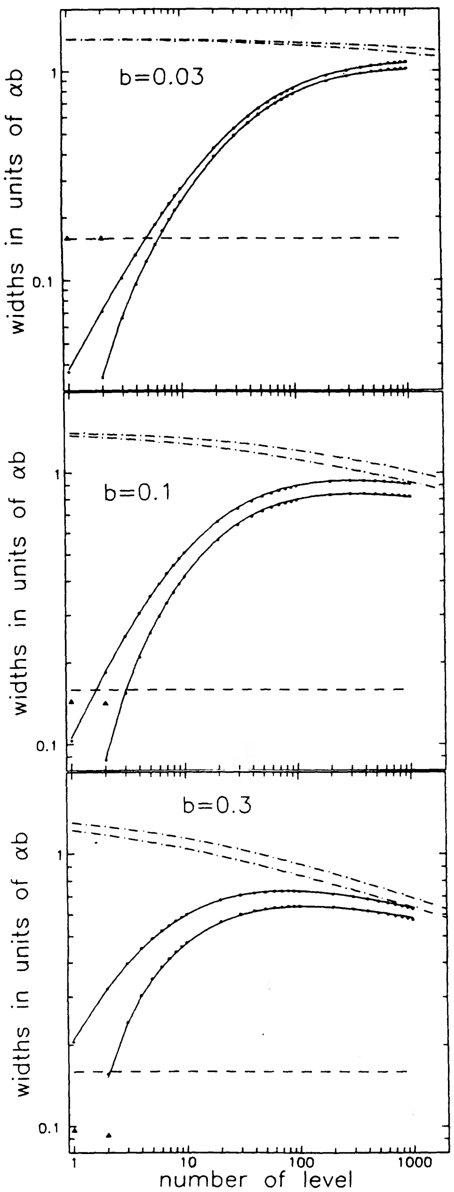

FIG. 1.—Dependence of the radiative widths $\Gamma_n^{-1}/\alpha b$ (*upper curve*) and $\Gamma_n^{+1}/\alpha b$ (*lower curves*) on the Landau level number n for three values of $b = B/B_Q$. The results of the numerical evaluation of eq. (3) are shown as dots; solid lines correspond to the interpolation formula (13), with coefficients given by eq. (14) and Table 2. Dashed-dot lines show the widths in the ultrarelativistic approximation of eq. (10). Dashed horizontal lines show the Schwinger value of the splitting, $\Delta\varepsilon/\alpha b = (2\pi)^{-1}$, and triangles mark the values of the splitting obtained from calculations of Geprägs et al. (1991).

TABLE 3

PARAMETERS $g_{i\zeta}$

ζ	$g_{1\zeta}$	$g_{2\zeta}$	$g_{3\zeta}$	$g_{4\zeta}$	$g_{5\zeta}$
−1..........	0.9451	−0.04383	1.752	0.196	7.628
+1..........	3.0868	0.42301	2.1654	0.57762	4.3276

For the first excited Landau level ($n = 1$) the previous fit by means of equations (13) and (14) is not so good. However, the widths Γ_1^ζ can be easily calculated with high accuracy, and the results can be fitted with the following expression:

$$\Gamma_1^\zeta = \frac{\alpha g_{1\zeta} b^{(5+\zeta)/2}}{[g_{2\zeta} + (1 + g_{3\zeta} b)^{g_{4\zeta}}]^{g_{5\zeta}}} . \tag{13a}$$

The fitting parameters $g_{i\zeta}$ to be used in equation (13a) are given in Table 3. The accuracy of this fit in the range $10^{-3} \leq b \leq 10^7$ is 0.55% for Γ_1^{-1} and 0.05% for Γ_1^{+1}, the results being shown in Figure 2.

3. RADIATIVE SPLITTING OF THE LANDAU LEVELS

From quantum electrodynamics, it is known that the radiative broadening of the discrete energy levels of a system is always accompanied by a radiative shift of the levels, the two quantities being related by dispersion relations. In the case of the Landau levels, the shift $\delta\varepsilon$ and the widths Γ are the real and imaginary part of the complex shift (e.g., Herold et al. 1982),

$$\delta\varepsilon_n^\zeta + i\Gamma_n^\zeta = \sum_k \frac{\langle i| H_I |k\rangle\langle k| H_I |i\rangle}{E_i - E_k + i0} , \tag{15}$$

where H_I is the interaction Hamiltonian, $|i\rangle$ is the initial state with one electron or positron of quantum numbers n and ζ, and $|k\rangle$ is an intermediate state with one electron or positron and one photon. A direct calculation of the real part is usually not simple because of divergences which need to be removed with an appropriate renormalization procedure (Geprägs et al. 1991). However, the quantities that are the most interesting are not the shifts themselves but the differences $\Delta\varepsilon_n = \delta\varepsilon_n^+ - \delta\varepsilon_n^-$, which give the energy splitting of the nth Landau level. This splitting was recognized by Sokolov & Ternov (1968) as being caused by the anomalous magnetic moment $\Delta\mu$ of the electron, the value of the splitting being

$$\Delta\varepsilon_n = \frac{\Delta\mu}{\mu_0} b , \tag{16}$$

where $\mu_0 = e\hbar/2m_e c$ is the Bohr magneton and $\Delta\mu$ depends generally on b and n.

The nature of the splitting can be understood more simply for nonrelativistic electrons. In this case the motion in a magnetic field is described by the Pauli equation

$$\left[\frac{(\boldsymbol{p} - e\boldsymbol{A}/c)^2}{2m_e} - \boldsymbol{\mu} \cdot \boldsymbol{B}\right]\Psi = E\Psi , \tag{17}$$

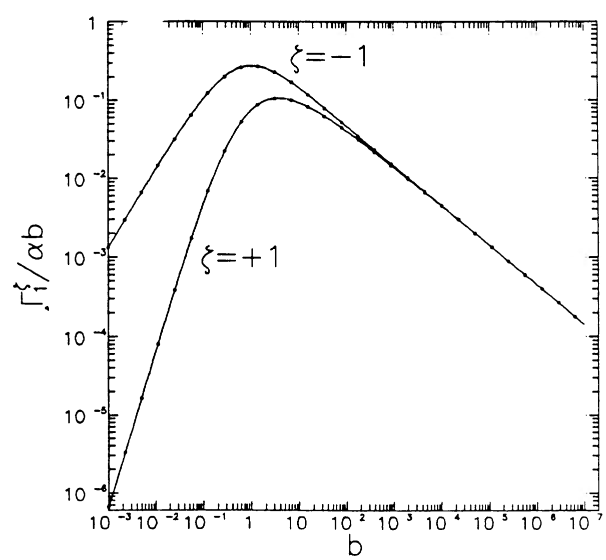

FIG. 2.—Dependence of the radiative width $\Gamma_1^\zeta/\alpha b$ as a function of b. Dots are the results of the numerical evaluation; solid lines are the values from the interpolation formula (13a) with the coefficients given in Table 3.

where $-\boldsymbol{\mu}\cdot\boldsymbol{B}$ takes into account the interaction of the spin magnetic momentum with the magnetic field, $\boldsymbol{\mu} = -\mu\boldsymbol{\sigma}$ is the magnetic moment operator, μ is the value of the magnetic moment, and $\boldsymbol{\sigma}$ is the spin operator. The eigenvalues of the nonrelativistic energy are given by

$$E = \hbar\omega_c\left(n_r + \frac{1}{2} + \frac{\zeta}{2}\frac{\mu}{\mu_0}\right) = \hbar\omega_c\left(n_r + \frac{1}{2} + \frac{\zeta}{2} + \frac{\zeta}{2}\frac{\Delta\mu}{\mu_0}\right), \tag{18}$$

where $n_r = 0, 1, 2, \ldots$ and $\zeta = \pm 1$. If $\mu = \mu_0$ (i.e., the anomalous magnetic moment $\Delta\mu$ is zero), the spin term either compensates the ground-state energy of the spinless electron $\hbar\omega_c/2$ or else it multiplies it by a factor of 2, giving thereby the nonrelativistic spectrum $E = n\hbar\omega_c$, with $n = n_r + 1$ for $\zeta = +1$ and $n = n_r$ for $\zeta = -1$. If, on the other hand, μ differs from μ_0, the spectrum turns into

$$E = \hbar\omega_c\left(n + \zeta\,\frac{\Delta\mu}{2\mu_0}\right), \tag{19}$$

i.e., the energy level with the spin-up electron ($\zeta = +1$) lies slightly higher than that for spin-down ($\zeta = -1$).

The anomalous magnetic moment for very low b was first calculated by Schwinger (1948) and is

$$\frac{\Delta\mu}{\mu_0} = \frac{\alpha}{2\pi} \qquad (b \ll 1,\ \eta \ll 1)\,. \tag{20}$$

The dependence of $\Delta\mu$ on n and b was analyzed by Sokolov & Ternov (1986), who obtained

$$\frac{\Delta\mu}{\mu_0} = -\frac{2\alpha}{\pi b}\sum_{n'=0}^{\infty}\int_0^{\infty} d\omega \int_0^{\pi/2} d\theta\, \frac{\omega\sin\theta}{[\varepsilon_{n'}(p_z') + \omega]^2 - \varepsilon_n^2}\left[1 + \frac{2(n'-n)b + \omega^2\sin^2\theta}{\omega\varepsilon_{n'}(p_z')\sin^2\theta}\right][I^2_{n,n'}(z) - I^2_{n-1,n'-1}(z)]\,, \tag{21}$$

where

$$\varepsilon_{n'}(p_z') = \sqrt{\varepsilon_{n'}^2 + \omega^2\cos^2\theta}\,, \qquad \varepsilon_n = \varepsilon_n(p_z = 0) = \sqrt{1 + 2nb}\,, \qquad z = \frac{\omega^2\sin^2\theta}{2b}\,,$$

and the $I_{n,n'}(z)$ are defined by equation (5). Equation (21) simplifies considerably in the previous limiting cases.

Case A: Nonrelativistic limit ($nb \ll 1$).—In this case $\Delta\mu$ is independent of n and differs only slightly from the Schwinger value (20), leading to a splitting:

$$\Delta\varepsilon_n = \frac{\alpha b}{2\pi}\left[1 - \frac{28b^2}{3}\left(\ln\frac{1}{b} - 1.446\right)\right] \simeq 0.16\alpha b\,. \tag{22}$$

In the opposite case of large $n \gg b^{-1} \gg 1$ (ultrarelativistic energies), the sum over n' in equation (21) can be replaced by an integral, and the quasi-classical expressions can be used for $I_{n,n'}(z)$. This yields (Sokolov & Ternov 1986)

$$\frac{\Delta\mu}{\mu_0} = \frac{\alpha\eta}{\pi}\int_0^{\infty}\frac{dv}{(1+\eta v)^2}\int_0^{\infty} dt\,\sin\left(t + \frac{4t^3}{27v^2}\right), \tag{23}$$

i.e., as for the radiative widths, the result depends on n and b only through the parameter η (eq. [10]). Therefore one can consider the same two following limiting cases below

Case B: Ultrarelativistic quasi-classical limit, $b^{-1} \ll n \ll b^{-3}$, ($\eta \ll 1$).—In this case equation (23) leads to approximately the same splitting as for $n \ll b^{-1}$, namely

$$\Delta\varepsilon_n = \frac{\alpha b}{2\pi}\left[1 - \frac{16}{3}\eta^2\left(\ln\frac{1}{\eta} - 1.55\right)\right] \simeq 0.16\alpha b\,. \tag{24}$$

Case C: Ultrarelativistic quantum limit, $n \gg b^{-3}$, ($\eta \gg 1$).—In this limit, the splitting decreases with increasing n:

$$\Delta\varepsilon_n = \frac{\alpha b\Gamma(1/3)}{9\sqrt{3}(2\eta)^{2/3}} \simeq \frac{0.074\alpha b}{(nb^3)^{1/3}}\,. \tag{25}$$

Equations (22), (24), and (25) can be combined in the interpolation formula

$$\Delta\varepsilon_n \simeq \frac{a_6\,\alpha b}{[1 + (a_7\,nb^3)^{a_8}]^{1/3a_8}}\,, \tag{26}$$

with $a_6 \simeq 0.16$, $a_7 \simeq 10.1$, and $a_8 = 0.5$, appropriate for the purposes of rough estimations.

Exact values of the shifts $\delta\varepsilon_n^\zeta$ were calculated by Geprägs et al. (1991) for $n = 1$ and $n = 2$ in a wide range of b. The corresponding splittings are shown by triangles in Figure 1. We see that for $b \lesssim 0.1$ the exact splittings are quite close to the Schwinger value of equation (20) (marked as a dashed horizontal line in Fig. 1), whereas for $b \gtrsim 0.1$ the exact values lie increasingly lower for increasing b.

4. DISCUSSION

Comparing the results of § 2 and 3, we see that the ratio of the cyclotron line splitting to the natural line width is approximately given by

$$\frac{\Delta\varepsilon_n}{\Gamma_n} \simeq \begin{cases} 0.12[(n-\frac{1}{2})b]^{-1} , & n \ll b^{-1} ; \\ 0.11 , & b^{-1} \ll n \ll b^{-3} ; \\ 0.057(nb^3)^{-1/6} , & n \gg b^{-3} . \end{cases} \tag{27}$$

Thus, in the nonrelativistic limit the interaction with the radiation field can remove the degeneracy of the lowest Landau levels satisfying

$$n < 0.5 + 0.12b^{-1} , \tag{28}$$

provided the field is not too strong, $b \lesssim 0.25$ (or $B \lesssim 10^{13}$ G). With decreasing field strength, the number of Landau levels which are nondegenerate increases. For instance, in a field $B \sim 3 \times 10^{12}$ G observed in the X-ray pulsar Her X-1 (Trümper et al. 1978; Mihara et al. 1990), only the first excited level can be considered sufficiently well split to be nondegenerate. However, in a field $B \sim 1 \times 10^{12}$ G, as observed in the X-ray pulsar 4U 0115+63 (White et al. 1983; Nagase et al. 1990), or $B \sim 2 \times 10^{12}$ G, as observed in the gamma-ray bursters GB 870303 and GB 880205 (Murakami et al. 1988), and the X-ray pulsar 4U 1358−52 (Clark et al. 1989), one may expect the splitting of two or three excited levels.

The amount of the splitting, in the nonrelativistic limit (22), is the same for all the levels independently of n:

$$\Delta E \simeq 0.6b \text{ keV} = 13.5(B/10^{12} \text{ G}) \text{ eV} . \tag{29}$$

This level splitting can, in principle, produce an observable substructure in the cyclotron resonance lines. If the resonance is associated with a transition $n \leftrightarrow 0$, the line should split into a doublet. The red component of the doublet arises due to spin-down $\leftrightarrow$ spin-down transitions, while the blue component (shifted by ΔE from the red component) arises from spin-flip transitions. If the resonance is associated with a transition between excited Landau levels, the line splits into a triplet, with the central component caused by spin-conserving transitions, while the red and blue satellites are caused by spin-down $\leftrightarrow$ spin-up and spin-up $\leftrightarrow$ spin-down transitions, respectively. The shift between the satellites equals $2\Delta E$.

In general, the observation of this superfine cyclotron structure in accreting X-ray pulsars and gamma-ray bursters should be difficult, since the splitting is very small compared to the line energy, and also compared to the typical line widths. However, they are, in principle, within the capabilities of modern high-resolution X-ray spectrometers. If the splitting exceeds the effects of all broadening machanisms, its observation at the first cyclotron harmonic $E \sim \hbar\omega_c$ would require a resolving power $R \geq \hbar\omega_c/\Delta E \simeq (0.16\alpha)^{-1} \simeq 860$. Such resolution is obtained with the XRS bolometer detector proposed for AXAF, or (at lower energies $\lesssim 3$ keV, if cyclotron lines are found there) also with high-dispersion gratings coupled to high spatial resolution imaging detectors, such as the BCS spectrometer. Several possible line-broadening mechanisms may be considered. One of these is the effect of magnetic field inhomogeneities. For a dipole field the radial extent of the line-producing region should not exceed $\Delta r/r \sim \alpha/6\pi \sim 4 \times 10^{-4}$ in order not to smear the split $\Delta\omega/\omega \sim \alpha/2\pi$, corresponding to $\Delta r \lesssim 400$ cm. The width of radiative shocks or the cooling region behind a collisionless shock in high-luminosity accreting pulsars may be larger than this, although the line need not necessarily form over the whole width. Alternatively, for accreting sources heated by Coulomb or nuclear collisions or for typical X-ray source thermal atmospheres, the width of the region could be well within the above constraint. There is also the variation of the dipole field with magnetic colatitude θ, $\Delta B/B \sim 3\theta^2/8$, which could smear out the lines if the size of the line region extends over a range of $\theta^2 > 4\alpha/3\pi \sim 3 \times 10^{-3}$. This is similar to the polar cap size $\theta^2 \sim 3 \times 10^{-3} L_{37}^{2/7} B_{12}^{-4/7}$ of accreting magnetized sources. However, radiative transfer calculations (e.g., Mészáros & Nagel 1985) indicate that the line forms over a depth which can be much smaller than the whole polar cap width. A more important broadening could be due to the Doppler effect, which gives a width $\Gamma_D \sim b(2T_* \cos^2\theta)^{1/2}$ for $T_* = kT/m_e c^2 \ll 1$ and $\cos\theta \gg \sqrt{T_*}$, or $\Gamma_D \sim bT_*$ for $\cos\theta \ll \sqrt{T_*}$, which exceeds the splitting for any θ if $T_* \gtrsim 0.16\alpha$ ($kT \gtrsim 0.6$ keV). If the optical depth τ in the wings is large, the actual line width could be larger than this by an additional factor of at most order a few, but in gamma-ray bursters one cannot exclude the possibility that the line formation region is thin or nearly thin, particularly at the harmonics above the first, e.g., as modeled by Miller et al. (1991).

The line shapes, however, become strongly asymmetrical for observation angles $\theta \to \pi/2$, with a sharp blue edge (see, e.g., Herold et al. 1982a; Bussard et al. 1986; Pavlov 1986; Bezchastnov & Pavlov 1990). This structure arises, on the one hand, due to a relativistic kinematical restriction on the maximum frequency of the emitted (absorbed) photon:

$$\omega < \omega_{\max}^{nn'} = \frac{\sqrt{1+2nb} - \sqrt{1+2n'b}}{\sin\theta} \to (n-n')b \qquad \text{at} \qquad nb \ll 1, \theta \to \frac{\pi}{2} , \tag{30}$$

and, on the other hand, due to the fact that at $\theta \to \pi/2$ the line is broadened only by the quadratic Doppler effect, which shifts the frequencies only toward the red wing (in the above units $\omega_c \equiv b$). The sharp blue edges are present also in the fine and superfine structure peaks, and their energy is constant, independent of temperature. This means that the superfine structure of the cyclotron lines may in principle be observable, even at high temperatures. This is because, no matter how broad the red wing of the line is, the blue edges will remain sharp and separate, if the field is sufficiently homogeneous and the line is observed close to perpendicular to the magnetic field. For the latter one does not require beaming in this direction, only an adequate phase angle resolution. The lines observed in accreting pulsars and gamma-ray bursters are believed to arise from cyclotron scattering, which causes an absorption-like feature. While scattering is a second-order process, the process can be approximated by that of a first-order cyclotron absorption followed by emission (e.g., Harding & Daugherty 1991), so the line shapes are similar. The fine-structure and hyperfine-structure splits discussed here will be essentially identical in the cyclotron scattering as in the cyclotron absorption, since the splits are given by the same mechanisms. We may therefore discuss these effects within the context of the first-order cyclotron process, neglecting for simplicity any transfer effects. The latter is clearly an oversimplification in accreting pulsars, but may be adequate for harmonics above the first in gamma-ray bursters. In this spirit, we may use the thin absorption profiles as a useful first-order description of the profiles that would be actually produced. The profile of the first harmonic of the cyclotron line $\omega \sim \omega_c$ due to $n - n' = 1$ transitions in a thermal plasma (calculated as described by Bezchastnov & Pavlov 1990) is plotted on the top half of Figure 3, showing the fine structure from individual $1 \rightarrow 0$, $2 \rightarrow 1$, $3 \rightarrow 2$, ..., transitions. The splitting is, of course, displayed either in the emission or the absorption profile, so for the usually observed absorption features one need simply consider the inverted form of Figure 3. The fine-structure peaks split further into a doublet (for the transition to the ground state $n' = 0$) or a triplet (for $n' = 1$, 2, ...). Two examples of this superfine-structure doublet and triplet for the first and second peak are shown qualitatively in the bottom half of Figure 3 (quantitative calculations will be given elsewhere). A similar picture applies to the higher harmonics $n - n' = 2, 3, \ldots$, as well. One should note that the red component of the doublet and the central component of the triplet, which are associated with spin-conserving transitions, are more intense than the spin-flip components.

The spin-conserving superfine transitions are not only more intense than the corresponding spin-flip transitions, they also have a different polarization. In the nonrelativistic approximation, the more intense components are associated with E1 (electric dipole) transitions, which contribute mainly to the extraordinary polarization mode, with the wave electric vector perpendicular to $\boldsymbol{B}$ at $\theta \rightarrow \pi/2$. The less intense spin-flip transitions, on the other hand, are associated mainly with M1 (magnetic dipole) transitions, which at $\theta \rightarrow \pi/2$ have an electric vector along the magnetic field (ordinary polarization mode). This means that the spectrum of the linear polarization degree should show a sharp jump when scanning from the blueshifted spin-flip components toward the spin-conserving main component. Such polarization features could be observed, in principle, with a narrow-band Bragg polarimeter, if the frequency of the cyclotron line falls in the instrumental sensitivity band (typically $\lesssim$4–5 keV, e.g., the Bragg device in the SXRP X-ray polarimeter array designed for the Spectrum X-Gamma mission). A detection could be made easier if it were possible to place the central frequency of the narrow-band polarimeter near the blue edge of the line and then one allowed the detection band to oscillate in frequency around the central position, which would produce a strong modulation of the polarization signal. This would help to identify the superfine structure with a polarization experiment.

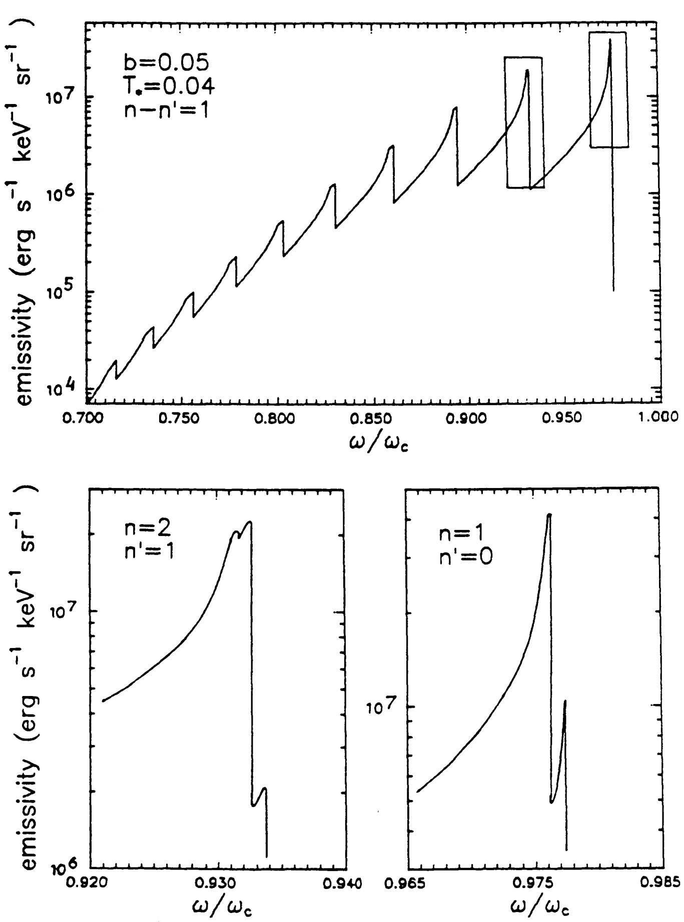

FIG. 3.—*Top*: spectrum of the first harmonic of the cyclotron radiative emissivity per electron for a thermal plasma with $T_* = 0.04$ ($kT \simeq 20$ keV), $b = 0.05$ ($B \simeq 2 \times 10^{12}$ G) at $\theta = \pi/2$. For the more commonly encountered absorption lines, neglecting transfer effects, the line profile would be given by this same figure upside down. Peaks in the spectrum (fine structure) are associated with transitions $n \rightarrow n - 1$ from different n. *Bottom*: qualitative picture of the doublet and triplet structure (superfine structure), imposed on the fine-structure peaks due to the splitting of the Landau levels, for the first two fine-structure peaks of the spectrum in the top of the figure.

Finally, it is worthwhile to point out that there may occur electron spin-flip transitions between the sublevels of the same Landau level, with typical frequency in the UV range ($\hbar\omega \sim$ 7–70 eV for $B \sim (0.5–5 \times 10^{12}$ G). The spontaneous rate of these transitions, however, should be much smaller than that of the X-ray transitions between different Landau levels (Parle 1986). If maser effects occur, which overpopulate the higher sublevel $\zeta = +1$ compared to the lower $\zeta = -1$, this could lead to a significant enhancement. This may occur for $n = 1$, because the $\zeta = +1$ level is depopulated by the less intense spin-flip transitions, while the $\zeta = -1$ is depopulated by the more intense spin-conserving transitions.

In summary, we have pointed out the possibility of distinguishing a superfine structure in the cyclotron lines of X-ray pulsars and gamma-ray bursters, if these are observed close to perpendicular to the field. These superfine doublets and triplets are caused by the anomalous magnetic moment of the electron in a strong field, and the components of the multiplets have different polarizations. Both the polarization and the amount of splitting, which depends on the magnetic field strength and Landau number, are in principle measurable, although not easily. Their detection would help determine the aspect angle under which a particular magnetic neutron star is observed and would strengthen the determination of the magnetic field strength by eliminating possible ambiguities in the harmonic number.

We are grateful to A. O. Golubeva and T. Bulik for computational assistance and R. Geprägs, H. Kaiser, H. Herold, and H. Ruder for communicating their results. This research has been supported in part through NASA NAGW-1522 and NSF AST 88-15266 and the Smithsonian visiting scientist program.

REFERENCES

Akhiezer, A. I., & Berestetckii, V. B. 1981, Quantum Electrodynamics (Moscow)
Bezchastnov, V. G., & Pavlov, G. G. 1990, Ap&SS, in press
Bussard, R., Alexander, S., & Mészáros, P. 1986, Phys. Rev. D, 34, 440
Clark, G., et al. 1990, ApJ, 353, 274
Daugherty, J., & Harding, A. K. 1986, ApJ, 209, 362
Geprägs, R., Kaiser, H., Herold, H., & Ruder, H. 1991, A&A, in press
Harding, A. K. 1986, ApJ, 300, 167
Harding, A. K., & Daugherty, J. K. 1991, ApJ, 374, 687
Harding, A. K., & Preece, R. 1989, ApJ, 338, L21
Herold, H., Ruder, H., & Wunner, G. 1982a, A&A, 115, 90
———. 1982b, Phys. Lett., 91A, 272
Latal, H. G. 1986, ApJ, 309, 372
Makishima, K., et al. 1991, ApJ, 365, L59
Mazets, E. P. 1981, Ap&SS, 80, 3
Melrose, D., & Zheleznyakov, V. V. 1981, A&A, 95, 86
Mészáros, P., & Nagel, W. 1985, ApJ, 299, 138
Mihara, T., et al. 1990, Nature, 346, 250
Miller, G. S., Epstein, R. I., Nolta, J. P., & Fenimore, E. E. 1991, Phys. Rev. Lett., in press
Mitrofanov, I. G., & Pozanenko, A. S., 1987, Soviet Phys.—JETP Lett., 93, 1951
Murakami, T., et al. 1988, Nature, 335, 234
Nagase, F., et al. 1991, ApJ, 375, L49
Parle, A. J. 1986, Ph.D. thesis, Physics Dept., University of Sidney
Pavlov, G. G. 1986, in Proc. Varenna-Abstumani Workshop Plasma Astrophysics (Paris: ESA), SP-251
Schwinger, J. 1948, Phys. Rev., 73, 416
Sokolov, A. A., & Ternov, I. M. 1968, Synchrotron Radiation (Berlin: Akademie)
———. 1986, Radiation from Relativistic Electrons (New York: AIP)
Trümper, J., et al. 1978, ApJ, 219, L105
Wheaton, W. A., et al. 1979, Nature, 282, 240
White, N., Swank, J. H., & Holt, S. S. 1983, ApJ, 270, 711
Yoshida, A., et al. 1990, in Proc. Taos Workshop on Gamma Ray Bursts, ed. R. Epstein, E. Fenimore, & C. Ho, in press